

Geophysical Research Letters, In Press.

Temperature and Pressure Dependent Kinetics of the Gas-Phase Reaction of the Hydroxyl Radical with Nitrogen Dioxide

Timothy J. Dransfield ¹, Katherine K. Perkins, Neil M. Donahue, and James G. Anderson,
Department of Chemistry and Chemical Biology, Harvard University, Cambridge, Massachusetts

Michele M. Sprengnether and Kenneth L. Demerjian
Department of Earth and Atmospheric Sciences, Atmospheric Sciences Research Center, SUNY, Albany

Abstract

The reaction of OH with NO₂ is pivotal in both stratospheric and tropospheric chemistry; in each case it is the dominant homogeneous mechanism for conversion of NO_x to NO_y. The rate constant is a strong function of pressure and temperature, and key portions of the pressure-temperature domain are poorly or ambiguously covered by the available data. These include conditions typical of the tropospheric boundary layer and of the lower stratosphere. At surface conditions differences of 60% exist both in the literature data and between the major recommendations, while at lower stratospheric conditions there are few available data. Our High Pressure Flow kinetics system is ideally suited to studying this reaction, as we are able to scan both temperature and pressure while maintaining wall-less conditions, eliminating the possible complications of heterogeneous chemistry. Here we report a temperature- and pressure-dependent study (220 - 300 K, 50 -150 torr) of this reaction; the measured rate constants are in excellent agreement with previously published values down to 240 K, but lie 10-20% lower than the historical data available below that temperature. An analysis of all available data motivates a large (~ 20%) downward revision in the recommended rate constant below room temperature.

¹Corresponding author

Introduction

The reaction of hydroxyl (OH) with nitrogen dioxide (NO_2) couples the odd-hydrogen and odd-nitrogen families in the troposphere and stratosphere [Johnston, 1971]. In the stratosphere it regulates the partitioning of both HO_x and NO_x between their active and reservoir forms, while in the troposphere it leads to irreversible HO_x and NO_x loss and also serves to bypass the ozone-production cycle [Wennberg et al., 1998].

In the mid to upper stratosphere, NO_x -catalyzed reactions comprise the dominant ozone loss mechanism. In the lower stratosphere, NO_x serves to inhibit the catalytic destruction of ozone by halogen and hydrogen radicals. NO_2 combines with the halogen radicals, BrO and ClO, to form the reservoir species, BrONO₂ and ClONO₂, while NO suppresses HO_2 , the rate-limiting radical in HO_x -catalyzed ozone loss [Stimpfle et al., 1994, Cohen et al., 1994]. Thus, ozone destruction rates can increase dramatically in low- NO_x conditions. To understand and predict the effects of anthropogenic activities on stratospheric ozone requires a complete and accurate representation of the mechanisms controlling odd-nitrogen chemistry. Understanding the partitioning of odd-nitrogen between the radical and reservoir species is especially important.

The partitioning between NO_x and NO_y is largely controlled by processes that effectively exchange NO_2 and HNO_3 , the dominant reservoir species. The gas-phase reaction of OH and NO_2 and the heterogeneous hydrolysis of N_2O_5 , BrONO₂, and ClONO₂ convert NO_2 to HNO_3 . NO_2 is released by HNO_3 photolysis and the reaction of HNO_3 with OH. In the lower stratosphere, the reaction of OH and NO_2 accounts for up to 95% of the total NO_2 to HNO_3 conversion, increasing in importance where the continuous sunlight suppresses N_2O_5 formation and thus the flux of molecules through the hydrolysis channel. When modeling odd-nitrogen chemistry, an overestimate of the rate of the title reaction at stratospheric temperatures and pressures will result in an underestimate of the abundance of NO_x .

As a termolecular radical recombination, this reaction depends on both temperature and pressure. The reaction product is thought to be nitric acid [Burkholder et al., 1987], though an additional stable isomer may be formed at low temperatures [McGrath and Rowland, 1994]. Accurate measurements of the rate constant and reaction products are therefore required from at least 175 to 325 K and 50 to 760 torr.

While the reaction has been studied extensively at room temperature, a large uncertainty remains at 760 torr and above. Most data and the JPL recommendation [DeMore

et al., 1997] do not agree with either the IUPAC recommendation [Atkinson et al., 1997] or the recent data of [Fulle et al., 1998], obtained in high pressures of He. The disagreement is severe, reaching 50% at standard temperature and pressure, and the implications for tropospheric ozone production are of corresponding consequence. For example, efforts to estimate ozone production efficiencies (OPE) and to model the long-range transport and distribution of NO_x in the atmosphere are dependent on lifetimes governed in large part by the rate of this reaction.

The dataset at subambient temperatures and atmospheric pressures is much less extensive, consisting of two experiments before this year [Anastasi and Smith, 1976, Wine et al., 1979], only one of which reached temperatures below 240K. Here we report measurements of this rate in a High Pressure Flow System (HPFS) at pressures of 50, 100 and 150 torr of nitrogen and over a temperature range from 218 K to 300 K. The concurrent study of [Brown et al., 1998] covers a similar range of pressures and temperatures. We discuss these data in the context of the JPL and IUPAC recommendations and provide a revised, temperature dependent recommendation for the pressure falloff parameters based on our earlier study at room temperature [Donahue et al., 1997]. While our understanding of the title reaction is now much improved, substantial uncertainties remain at temperatures below 220 K and pressures above 200 torr.

Experimental

Our High Pressure Flow System (HPFS) has been extensively described in the literature. The fluid dynamics of the ‘core flow’ conditions have been described analytically [Donahue et al., 1996], and we have obtained high-accuracy results from 2 to 600 torr (e.g. Donahue et al., 1997) and from 175 to 400 K (e.g. Clarke et al., 1998). The HPFS is designed to satisfy the following experimental objectives: (a) the careful control of radical production, (b) the maintenance of defined flow character, either laminar or turbulent, (c) the isolation of the reaction zone from the wall, and (d) the direct observation of axial and radial concentration derivatives. Taken together, these objectives provide high-accuracy discharge-flow kinetics data over the full temperature and pressure range of the atmosphere. Radicals in the HPFS do not come into contact with the tube walls, and highly sensitive radical measurements allow operation at low radical number density even at elevated pressures. Therefore, homogeneous and heterogeneous chemical interferences are largely eliminated.

In this experiment, NO_2 (1% in He, Matheson) is injected far upstream (7 m) and introduced into the center of

a 10 m/s flow of N_2 carrier gas. Hydroxyl radicals are generated via the titration reaction $H + NO_2 \rightarrow OH + NO$ in a sidearm radical source and then injected into the center of the flow roughly 50 cm upstream of the detection region, where the concentration of OH is measured using LIF at 5 locations along the flow tube.

Some modifications have been made to the cooling procedure for the present study. Cooling of the flow tube is now accomplished by replacing a fraction of the N_2 carrier gas with liquid nitrogen injected directly into a settling chamber. The liquid evaporates rapidly to produce a stable flow of carrier gas, while quickly (within 20 minutes) cooling the system to a stable temperature. After a series of experiments are conducted at a given temperature, the ratio of gaseous to liquid N_2 is changed, and equilibrium is obtained at a different temperature. The current operational range is ~ 200 - 400 K at 50 torr, and ~ 230 - 400 K at 150 torr. This allows us to study a range of pressures and temperatures relevant to the upper troposphere and lower stratosphere. A combination of reduced OH sensitivity and reduced thermal stability prevents operation above 150 torr at reduced temperatures. Modifications are currently in progress to expand the operational range of the experiment to conditions typical of the lower troposphere.

Mixtures of NO_2 and a passive tracer, CF_2Cl_2 , allow us to monitor the reagent concentration by three methods: FTIR absorption of the tracer and the NO_2 , and UV absorption of the tracer at 1849\AA . Under most conditions, reagent concentrations determined by these methods agree to within 5%; the results reported here are based on FTIR measurement of the tracer, which has the highest precision. Reagent mixing ratios are known to better than 5%. Velocity is measured with a pitot-static tube situated at the end of the OH detection zone, while temperature is measured with thermistors located at the pitot-static tube and at the radical injector. The accuracy is approximately 5% at room temperature, decreasing to 10% at 200K, being limited by the concentration of NO_2 at room temperature and by the velocity measurement at low temperatures [Donahue et al., 1998]. As a final measure of accuracy, we alternated measurements of the title reaction with measurements of the well-studied reactions OH + ethane and OH + cyclohexane. Both rate constants agreed with earlier measurements at all pressures over the entire temperature range of the study.

Results

We conducted three sets of experiments, at 50, 100, and 150 torr of N_2 , from roughly 220K to 300K. The experi-

Table 1. Rate constants for OH + NO_2 vs. temperature and pressure of N_2 . Units are $10^{-12} \text{ cm}^3 \text{ molecule}^{-1} \text{ s}^{-1}$. The number of runs under each condition is shown in parentheses. Uncertainties are 1- σ precisions.

T (K)	50 torr	100 torr	150 torr
212.5	(5) 6.08 ± 0.31	-	-
225	(2) 5.64 ± 0.31	(6) 7.76 ± 0.45	-
237.5	(4) 4.55 ± 0.38	(3) 6.49 ± 0.77	(6) 8.19 ± 0.43
250	(3) 3.73 ± 0.23	(4) 5.84 ± 0.30	(9) 6.82 ± 0.37
265	-	(5) 4.63 ± 0.36	(3) 5.81 ± 0.33
295	(1) 2.11 ± 0.07	(2) 3.62 ± 0.13	-
310	-	-	(1) 3.78 ± 0.12

ments were carried out with NO_2 concentrations between $2 \times 10^{12} \text{ cm}^{-3}$ and $7 \times 10^{12} \text{ cm}^{-3}$ and initial OH concentrations of approximately $2 \times 10^{10} \text{ cm}^{-3}$. Pseudo first-order conditions were maintained at all times. The resulting rate constants were binned and averaged according to temperature and pressure, and the results are shown in Table 1. In Figure 1 we show our data, along with the results of previous studies of this reaction and the recommendations of the JPL and IUPAC panels.

Discussion

The low-temperature results presented here may be directly compared with two earlier studies [Wine et al., 1979 and Anastasi and Smith, 1976], and one [Brown et al., 1998] conducted concurrently with this work; in general, there is excellent agreement among these studies. The agreement is better than 10% over most of the pressure and temperature domain, with the exception of [Anastasi and Smith, 1976] at 220K in N_2 . Those data appear to be systematically high by $\sim 20\%$; they strongly influence the current recommendations, which overestimate the rate constant by between 20 and 30% below 250 K.

As discussed previously [Donahue et al., 1997], the temperature- and pressure-dependent rate constant is well characterized by the pressure fall-off model of Troe [Troe, 1979]. The simplified forms used by the IUPAC and JPL panels can describe a subset of the data, but fail outside of that limited range. The data we use for fitting are the same used by [Donahue et al., 1997], with the addition of our data and that of [Brown et al., 1998]. We first fit the data at 298K as a function of pressure, then fit data below 500 K, allowing only the low-pressure exponent to vary. While we cannot fit the high-pressure measurements of [Fulle et al., 1998], we see no reason to reject their conclusion that the high-pressure rate constant is independent of temperature. The resulting function and parameters follow:

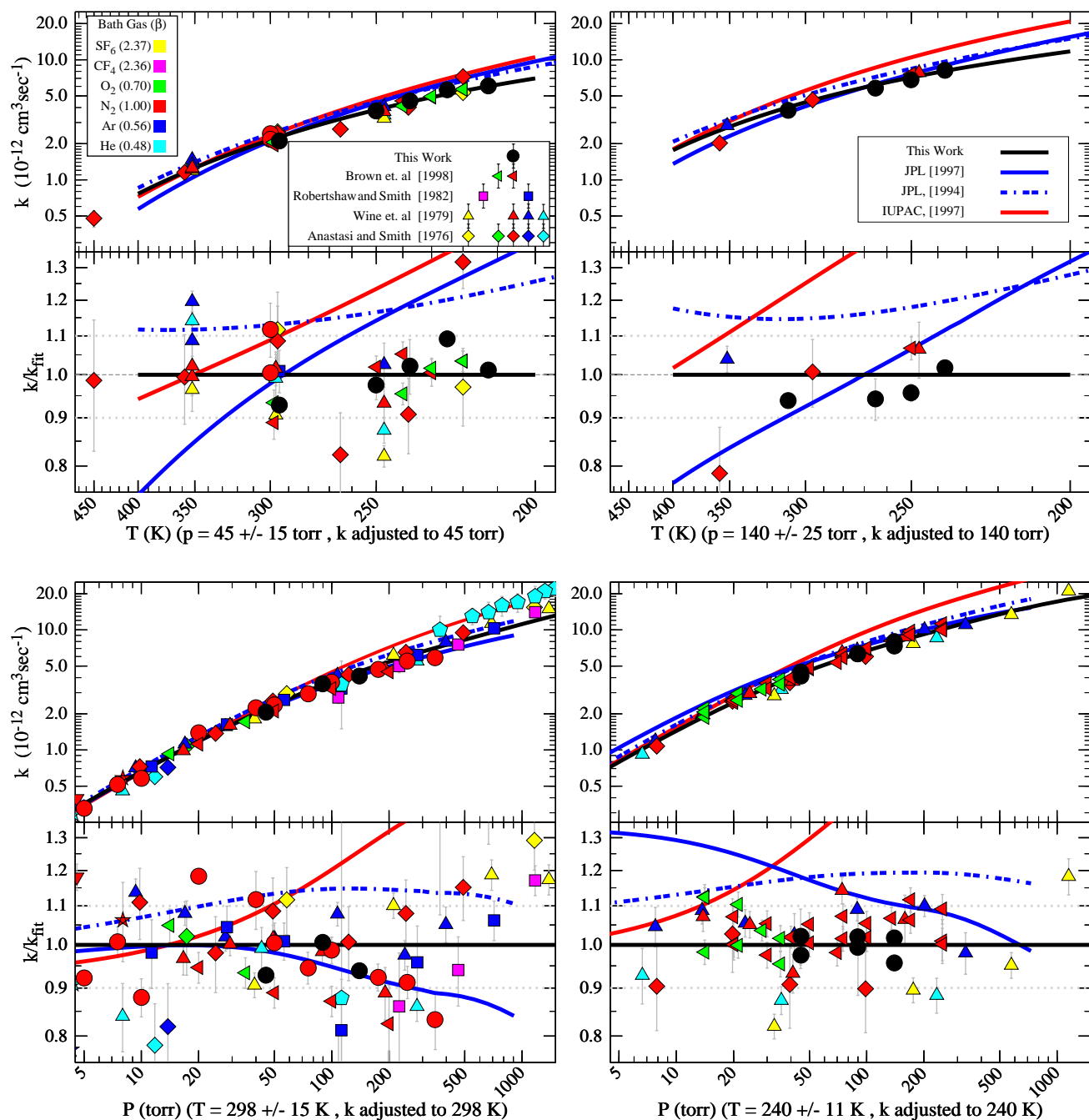


Figure 1. Data for the reaction $\text{OH} + \text{NO}_2 \rightarrow \text{products}$ as a function of pressure and temperature. Our data are plotted as solid black dots. Literature data are also shown, with different carrier gases represented by differing symbol colors. Symbol shapes identify the study responsible for each datum, as show in the legend; the red symbol color indicates nitrogen carrier gas (with the exception of our data, which are shown as solid black for emphasis). Pressures for bath gases other than N_2 are scaled by the collisional efficiency indicated in the legend. The latest IUPAC and JPL recommendations are shown as red and blue curves, while previous versions of these recommendations are shown as dashed curves of the same color. Our recommendation is shown as a black curve. The lower panel of each graph shows the ratio of each value to our recommendation.

$$k = k_0 \left(\frac{\beta_i[M]}{1 + \beta_i[M]/[M]_c} \right) F(\beta_i[M]/[M]_c)$$

$$F(\beta_i[M]/[M]_c) \simeq F_c^{1/B(\beta_i[M]/[M]_c)}$$

$$B \left(\frac{\beta_i[M]}{[M]_c} \right) \simeq 1 + \left[\frac{\log(\beta_i[M]/[M]_c) - 0.12}{N + \Delta N} \right]^2$$

$$N \simeq 0.75 - 1.27 \log(F_c)$$

$$\Delta N \simeq 0.1 + 0.6 \log(F_c), (\beta_i[M]/[M]_c > 1)$$

$$\Delta N \simeq -(0.1 + 0.6 \log(F_c)), (\beta_i[M]/[M]_c < 1)$$

$M_c = k_\infty/k_0$, $k_0 = 2.85 \times 10^{-30} (T/300)^{-2.67} \text{ cm}^6/\text{sec}$, $k_\infty = 3.13 \times 10^{-11} \text{ cm}^3/\text{sec}$, $F_c = e^{-T/T_c}$, $T_c = 363 \text{ K}$. We continue to use a ‘semi-strong’ collisional assumption, in which β scales with bath gas number density. For these data $\beta_{N_2} = 1$ and $\beta_{O_2} = 0.7$, with other bath gases shown in the figure legend. This function yields rates in N_2 of $4.61 \times 10^{-12} \text{ cm}^3/\text{sec}$ at 240 K, 50 torr and $9.94 \times 10^{-12} \text{ cm}^3/\text{sec}$ at 298 K, 760 torr.

This function is plotted in figure 1 and serves as the reference for the residuals plotted in the lower panels. Most of these residuals are <10%; however, below 220 K the rate constant is unconstrained, and extrapolation is perilous. There is also a substantial uncertainty at room temperature and pressure. The existing data in N_2 differ by ~30%, and the IUPAC and JPL recommendations differ by 60%.

Conclusions

These results significantly decrease the uncertainty in this rate constant under conditions typical of the upper troposphere and lower stratosphere. The roughly 20% reduction in the rate constant from the JPL97 recommendation will produce a commensurate increase in modeled NO_x/NO_y in the lower stratosphere. Furthermore, these data reinforce our earlier conclusion that the room temperature rate constant is well represented by the function we provide here. However, critical portions of the pressure-temperature domain remain under constrained; these include high pressures at room temperature and upper tropospheric and stratospheric pressures (<200 torr) at very low temperatures (175-225K).

Acknowledgements

This work was funded by grants from NSF and US EPA.

References

- Anastasi, C. and Smith, I. (1976). Rate measurements of reactions of OH by resonance absorption. *Journal of the Chemical Society, Faraday Transactions*, 2:1459.
- Atkinson, R., et al. (1997). Evaluated kinetic and photochemical data for atmospheric chemistry. supplement VI. IUPAC subcommittee on gas kinetic data evaluation for atmospheric chemistry. *J. Phys. Chem. Ref. Data*, 26:1329.
- Brown, S. S., Talukdar, R. K., and Ravishankara, A. (1998). Rate constants for the reaction $OH + NO_2 + M \rightarrow HNO_3$ under atmospheric conditions. *Chem. Phys. Lett.*, In Press.
- Burkholder, J., Hammer, P., and Howard, C. (1987). Product analysis of the $OH + NO_2 + M$ reaction. *J. Phys. Chem.*, 91:2136.
- Clarke, J., Kroll, J., Donahue, N., and Anderson, J. (1998). Testing frontier orbital control: OH + ethane, propane, and cyclopropane from 180 K to 360 K. *J. Phys. Chem.*, 102:9847.
- Cohen, R., et al. (1994). Are models of catalytic removal of O_3 by HO_x accurate? constraints from in situ measurements of the OH to HO_2 ratio. *Geophys. Res. Lett.*, 21:2539.
- DeMore, W. B., et al. (1997). Chemical kinetics and photochemical data for use in stratospheric modeling. Technical Report 97-4, Jet Propulsion Laboratory.
- Donahue, N. M., Clarke, J. S., Demerjian, K. L., and Anderson, J. G. (1996). Free radical kinetics at high pressure: A mathematical analysis of the flow reactor. *J. Phys. Chem.*, 100:5821.
- Donahue, N. M., Demerjian, K. L., and Anderson, J. G. (1998). New rate constants for ten OH alkane reactions from 300 to 400 K: An assessment of accuracy. *J. Phys. Chem.*, 102:3121.
- Donahue, N. M., et al. (1997). A high pressure flow study of the reactions $OH + NO_x \rightarrow HONO_x$: Errors in the falloff region. *J. Geophys. Res.*, 102:6159.
- Fulle, D., Hamann, H. F., Hippler, H., and Troe, J. (1998). Temperature and pressure dependence of the addition reactions of HO to NO and to NO_2 . IV. saturated laser-induced fluorescence measurements up to 1400 bar. *J. Chem. Phys.*, 108:5391.

- Johnston, H. (1971). Reduction of stratospheric ozone by nitrogen oxide catalysts from supersonic transport exhaust. *Science*, 173:517.
- McGrath, J. and Rowland, F. (1994). Determination of the barriers to internal rotation in ONOOX (X=H,Cl) and characterization of the minimum energy conformers. *J. Phys. Chem.*, 98:1061.
- Stimpfle, R., et al. (1994). The response of ClO radical concentrations to variations in NO₂ radical concentrations in the lower stratosphere. *Geophys. Res. Lett.*, 21:2543.
- Troe, J. (1979). Predictive possibilities of unimolecular rate theory. *J. Phys. Chem.*, 83:114.
- Wennberg, P., et al. (1998). Hydrogen radicals, nitrogen radicals, and the production of O₃ in the upper troposphere. *Science*, 279:49.
- Wine, P., Kreutter, N., and Ravishankara, A. (1979). Flash photolysis resonance fluorescence kinetics study of the reaction OH + NO₂ + M → HNO₃ + M. *J. Phys. Chem.*, 83:3191.